A Mathematical Model for Germinal Centre Kinetics and Affinity Maturation

Dagmar Iber*and Philip K. Maini
Mathematical Institute, 24-29 St Giles, Oxford OX1 3LB

November 20, 2001

Abstract We present a mathematical model which reproduces experimental data on the germinal centre (GC) kinetics of the primed primary immune response and on affinity maturation observed during the reaction. We show that antigen masking by antibodies which are produced by emerging plasma cells can drive affinity maturation and provide a feedback mechanism by which the reaction is stable against variations in the initial antigen amount over several orders of magnitude. This provides a possible answer to the long-standing question of the role antigen reduction has in driving affinity maturation. By comparing model predictions with experimental results, we propose that the selection probability of centrocytes and the recycling probability of selected centrocytes are not constant but vary during the GC reaction with respect to time. It is shown that the efficiency of affinity maturation is highest if clones with an affinity for the antigen well above the average affinity in the GC leave the GC for either the memory or plasma cell pool. It is further shown that termination of somatic hypermutation several days before the end of the germinal centre reaction is beneficial for affinity maturation. The impact on affinity maturation of simultaneous initiation of memory cell formation and somatic hypermutation versus delayed initiation of memory cell formation is discussed.

Running Headline: *A Model for GC Kinetics*

1 Introduction

Affinity maturation refers to the increase in affinity of the antibodies for antigen produced during the course of an immune response [16]. This is achieved by mutation of the genes encoding for the antibody and subsequent selection of those B cells which express B cell receptors with the highest affinity for antigen [27]. How mutation and selection are regulated is currently unknown. Both processes are believed to take place in the germinal centres of secondary lymphoid organs [4, 14].

Upon immunisation (infection) the antigen is concentrated in the secondary lymphoid organs where a small subset of all B cells recognise it [8]. After successful presentations of antigen fragments to T cells, B cells enter the blast state [27]. A subset of the antigen specific B and T cells enter the follicle and continue dividing about 4 times a day [24]. After about 3 days B blasts differentiate into centroblasts which still divide every 6-7 hours and after 4 days a spatial reorganisation can be observed. It has been shown that centrocytes are the progenitors of centroblasts

*Author for correspondence: Present address MRC-LMB, Hills Road, Cambridge CB2 2QH, di205@cam.ac.uk

[24]. Centrocytes express B cell receptors on their surface and are believed to be subject to selection by antigen in the form that they need to bind, internalise and present antigen to T cells [21] in order not to undergo apoptosis [25]. Those centrocytes that successfully interact with T cells can either differentiate into memory or plasma cells [25]. There is accumulating experimental evidence for a third differentiation pathway back into the centroblast state [7, 9, 24].

Soon after the first differentiation of centroblasts into centrocytes, somatic hypermutation starts to act on centroblasts and leads to a change in the affinity of the B cell receptors for antigen. About half of the mutations (53%) have been estimated to be of a silent nature not leading to any change in affinity [34]. About 28% have been estimated to lead to B cell death which is in good agreement with the apoptotic cells observed in the dark zone where centroblasts proliferate [11, 24]. 19% of all mutations have been estimated to have an effect on affinity. This effect can either be of an improving nature and drive affinity maturation, or of worsening or specificity changing character which may even lead to the formation of autoreactive clones. Selection is therefore clearly needed. It is currently unclear how exactly the read-out may work. Several studies support the concept that antigen is presented on the surface of follicular dendritic cells (FDCs) [23] and that this membrane presentation may lower the affinity threshold [3] and the required amount of deposited antigen [2] such that early clones of low affinity can also successfully extract and present antigen. The threshold needs to be dynamic with respect to time in order to drive affinity maturation. This dynamic nature may derive from increasing competition between centrocytes for free antigen which is probably reduced by antigen extraction [2] and masking through antibodies produced by early plasma cells [33, 39]. In Table 1, we summarise the key stages of the primed primary immune response.

How activation of B cells by antigen and T cells determines their fate, for example, whether they differentiate into either centroblasts, memory or plasma cells, is currently unknown and there is no experimental system available to investigate this. A mathematical model is therefore helpful for investigating hypotheses and checking their compatibility with available data.

Before investigating affinity maturation we first need to construct a model of the germinal centre (GC) kinetics which reproduces all experimental data on the GC reaction. Into this model the model of affinity maturation can then be embedded. Previous mathematical models of the process were very complex and unable to reproduce all data on the germinal centre reaction. An important condition for being able to construct a good model is the availability of a large body of reliable experimental data. The model presented below is therefore constructed for the primed, instead of for the true, primary immune response, since more (and also more accurate) data are available for the former. In the primed primary immune response an animal is first immunised with a precipitated carrier protein that activates T cells. A month later the animal is again immunised with the carrier protein but this time it is conjugated to a hapten. A hapten is an agent that is too small to raise an immune response but, when conjugated to a carrier protein, it is recognized by the immune system and raises an immune response. Importantly, the hapten-carrier protein complex can be injected in soluble form. This leads to a faster clearance of the antigen from the body and a sharper response which allows a more accurate description of the process and therefore yields better data. The problem of modelling the true primary immune response already begins with deciding on the exact time of onset of the immune response, since this is smeared over a time span of several days because the antigen needs to be injected in precipitated form and dissolves slowly. A drawback of modelling the primed instead of the true primary

immune response is that due to the priming, T cell help is non-limiting and the immune response against the hapten is faster and stronger than in the unprimed case. This is an unfortunate side effect since the mechanisms of the two responses may therefore be different and an understanding of the artificial primed primary immune response does not directly imply an understanding of the true primary immune response. Many features will however be similar although the kinetics differ [24] and an understanding of the primed primary immune response may therefore facilitate an understanding of the true primary immune response. In the following a simplistic mathematical model is devised with which all available data can be reproduced and predictions can be made concerning selection strategies and the regulation of the differentiation of selected centrocytes into either memory, plasma cells or centroblasts.

2 The basic model

Calculations based on the emergence of antigen specific B cells led to the suggestion that follicles are seeded during the first hours of infection (immunisation in experiments) and that each follicle soon becomes dominated by five (or fewer) clones [12, 19, 24]. In the model it is therefore assumed that the GCs are seeded by three clones which give rise to 12288 B blasts within three days if we use the proliferation rate $\rho = \frac{24}{6.5} \ln 2 \text{ day}^{-1}$ for centroblasts determined by Liu and coworkers [24]. At day 3, B blasts differentiate into centroblasts and the main GC reaction starts. The model, presented schematically in Figure 1, takes the form

$$\frac{dB}{dt} = p_r \rho C_s - \rho B \tag{1}$$

$$\frac{dC}{dt} = 2\rho m B - \mu C \qquad \text{with} \quad \mu = ds + \delta_c(1-s) \tag{2}$$

$$\frac{dC_s}{dt} = dsC - \rho C_s \tag{3}$$

$$\frac{dM}{dt} = (1-p_r)\rho C_s \tag{4}$$

and is derived in the following way. There is no experimental work on the regulative mechanism for differentiation of centroblasts into centrocytes. In a previous model, Kesmir and de Boer [18] assumed that centroblasts differentiate into centrocytes after a set number of generations n, which is larger than 4. One can show that other mechanisms, such as time dependent or cell density dependent centroblast-centrocyte conversion, cannot satisfy all experimental data. In this model we will therefore also assume generation-dependent centroblast differentiation but it will be shown later that agreement with the experimental observations of MacLennan and coworkers [28] only occurs if we assume that centroblasts already differentiate into centrocytes after one cell division.

The conversion of centroblasts into centrocytes could involve only one or both daughter cells. However, in the former case we would not obtain the observed GC kinetics since the centroblast pool could only increase but not decrease since no net outflux term would be included and the GC reaction would never terminate. Hence, in the model it is assumed that centroblast division directly leads to differentiation of both daughter cells into centrocytes and we therefore have the term $-\rho B$ in equation (1). Due to somatic hypermutation only the proportion m survives the cell division and differentiates into centrocytes while the remaining proportion $(1-m)$ of dividing centroblasts is assumed to die at the same rate as the surviving part differentiates. The death rate of centroblasts may well be smaller than the conversion rate. Such

a possible difference cannot however be expected to change the modelled kinetics substantially if we assume that centroblasts, once committed to apoptosis, can not take part in the normal cell division process. A smaller death rate would therefore only lead to a slower decay of the total cell number. The surviving centroblast proportion gives rise to the term $2\rho mB$ in equation (2). The factor 2 comes in since one centroblast gives raise to two centrocytes and division of centroblasts is assumed to lead directly to differentiation into centrocytes.

Part of the centrocyte population (sC) becomes selected into the pool C_s at a rate d [24] via interaction with antigen and T cells (whose dynamics are not included in this first simple model). This generates the term dsC in equation (3). The other part ($(1-s)C$) undergoes apoptosis with rate δ_c [28] and the outflux from the centrocyte pool is therefore in total $(ds+\delta_c(1-s))C$, which is written as μC in (2). The selected centrocytes (C_s) can then take either of two routes: they may, with probability $(1-p_r)$, differentiate into memory (M) or antibody forming plasma cells (AFC) (at this stage we do not differentiate between these two cell types and denote both populations by M); or they may, with probability p_r, recycle and replenish the centroblast pool. The time needed to recycle is assumed to be, on average, about 6 hours and therefore we again use ρ as a rate constant, leading to the term $p_r\rho C_s$ in (1). We further assume that selected centrocytes differentiate at the same rate into memory or plasma cells as they recycle so that the net outflux term from the pool of selected centrocytes is given by $-\rho C_s$ in equation (3). By the same argument, the influx into the memory pool (4) is given by $(1-p_r)\rho C_s$. A different efflux rate from the GC would only change the total number of cells fluxing into the memory and plasma cell pool. Both numbers are currently unknown and difficult to measure since both memory and plasma cells emigrate from the follicles and are then difficult to track.

Non-dimensionalisation of the model does not lead to any new insight since the form of the equations remains unchanged (that is, there are no small parameters that we can exploit). We note that the M equation is decoupled from the rest of the system so we analyse the first three equations of the model system. This system always has a trivial equilibrium point. A non-trivial equilibrium point exists if

$$\mu = \mu_c = 2p_r msd. \tag{5}$$

At the equilibrium point s therefore takes the value

$$s_c = \frac{\delta_c}{d(2p_r m - 1) + \delta_c}. \tag{6}$$

Given that the selection factor s can only take values between 0 and 1 in the model, we obtain as a further condition on the denominator

$$p_r m \geq 0.5 \tag{7}$$

in order to attain the equilibrium state within the possible parameter space. Due to somatic hypermutation the survival rate m has been calculated to be about 0.72 [34] or 0.75 [1]. Other sources are more pessimistic and consider $m = 0.5$ [17]. For the latter parameter value of m we would need $p_r = 1$ in order to meet condition (7). p_r however cannot attain the value 1 since then no memory cell formation would be possible (4). We therefore have $m > 0.5$ as a necessary condition for a non-trivial equilibrium state. For $m \leq 0.5$ we have $\mu > \mu_c$ for all parameters in the parameter space. Simple analysis shows that the solution blows up for $\mu < \mu_c$ while for $\mu > \mu_c$ it tends to the trivial equilibrium point. If we use $m = 0.72$ on the other hand, we only need $p_r \geq 0.69$ in order to attain a non-trivial equilibrium state.

3 Results and predictions

3.1 Without termination of somatic hypermutation at day 16 no enhancement in the stringency of selection is needed

Experimental observations show that the overall shape of the GC kinetics during the primed primary immune response [24] is characterised by an exponential increase in cell numbers until day 3 or day 4, when the number of cells reaches about $1-1.5\times10^4$ [20, 24], followed by a halving of cell numbers until day 7. After day 7 cell numbers decline more slowly until the GC reaction finishes at about day 21 [24].

In order to model the decrease in cell numbers we have to determine the set of parameters for which the model attains the trivial equilibrium state. From the analysis of the system we conclude that this happens when s and p_r are small. It is generally believed that the decrease in cell population during the GC reaction is mainly due to non-selected centrocytes which are dying [27]. It is further believed that selection is critically dependent on the amount of available antigen, which can be reduced during the reaction by antigen extraction [2] and antigen masking through soluble antibody produced by early plasma cells [33, 39]. From the latter it follows that the value of the selection factor will only decrease during the GC reaction. The weaker decrease in cell numbers after day 7 must therefore be due to the increase of the other undetermined parameter, the recycling probability p_r. This assumption can be justified by the experimental result that early clones of high affinity have been observed to preferentially leave the GC reaction. We will come back to this point later. At this stage it is sufficient to assume that those centrocytes which receive a very strong activation signal compared to the average centrocyte population preferentially leave the GC reaction. Given that B cell and subsequent T cell activation (interleukin-2 production) is dependent on the availability of antigen [2], and given further that the curve of T cell activation as a function of antigen density is of sigmoidal shape [2], the behaviour can best be modelled by the use of a Hill function. We use

$$p_r = 0.6 + 0.2\frac{Ag^n_{min}}{Ag^n + Ag^n_{min}} \tag{8}$$

where Ag is antigen density, $Ag_{min} = 7500$ and $n = 50$. The parameters Ag_{min} and n are chosen such that the experimental kinetics can be reproduced.

The amount of unbound antigen decreases during the GC reaction due to antigen consumption and masking by high affinity soluble antigen. The latter will be included once we have modelled affinity maturation. At this stage we only consider antigen reduction by extraction through centrocytes. The initial number of antigen complexes in the lymph node has been estimated to be 5×10^8 [40] although this number will vary between immune responses [26]. Given that every GC consists of about 1.5×10^5 cells and every spleen of about $5-7\times10^7$ cells, the number of GCs can be estimated to be about 300-500. So there are at least 10^6 antigen molecules per GC. If we follow the estimate in [18] there are 100 FDCs per GC and therefore on average 10^4 antigen molecules per FDC.

The natural decay of antigen is more or less irrelevant since this natural decay is much slower than all active processes. The antigen decay is therefore probably mainly due to antigen extraction by centrocytes. It is sensible to assume that there is more extraction the more centrocytes interact with antigen and the higher the antigen density on FDCs since this may facilitate extraction. Assuming further, for simplicity, a linear influence we are left with $-uC_sAg$ as the term modelling the extraction by selected centrocytes where Ag is the antigen density. Given that centrocytes which do not manage to become selected may extract antigen as well

we also need to take this proportion of non-selected centrocytes into account. This cell proportion is taken to be $k(C - C_s)$ and we therefore obtain the second term modelling the antigen dynamics to be $-uk(C - C_s)Ag$ yielding in total for the antigen dynamics

$$\frac{dAg}{dt} = -(ukC + uC_s(1-k))Ag. \tag{9}$$

Since k is not known from experiments we assume, for simplicity, that $k = 0$. We can easily change this once experimental data are available but, given that u and the initial and final antigen density are unknown it does not seem appropriate to explore k at this stage. There is no evidence in the literature that the antigen consumption rate depends on the quality of BCR:antigen interaction and u is therefore taken to be constant. The exact value of $u = 2.5 \times 10^{-5}$ was chosen with the result in mind that within thirty days about half of the antigen has disappeared from the lymph nodes [40]. Hence there is still a lot of antigen available in the lymphoid organs when the GC reaction terminates and lack of antigen is therefore unlikely to be the primary reason for GC termination (as proposed previously [18]). An alternative model [30] proposes that GC termination is due to emigration of GC B cells as memory or plasma cells and this is the view that we will take. In the model of affinity maturation we will see how antigen masking can affect selection and emigration which finally leads to GC termination. The results for this model can be seen in the top panel of Figure 2. The total number of B cells peaks at day 4 with about 1.2×10^4 B cells. This is in good agreement with the experimental results of Liu and coworkers [24]. MacLennan and coworkers find that centrocytes greatly outnumber centroblasts during the main part of the GC reaction and this is also found in the model results. We conclude from the results shown in Figure 2 that it is sufficient to assume that the recycling rate can change with respect to time - while the selection factor can be kept constant ($s = 0.28$) - in order to reproduce the experimental kinetics of the GC reaction.

Jacob and coworkers [15] deduced from their experimental results that either the selection stringency has to increase or somatic hypermutation has to terminate at about day 16. It is possible to enhance selection stringency (reduce s) in this model and still to reproduce the experimental kinetics (data not shown) but there is nothing that would justify this. If however somatic hypermutation terminated at day 16 (as was proposed in [4]) then the somatic hypermutation survival rate would increase from $m = 0.72$ to $m = 1$. From (6) we see that s_c decreases when m increases. Upon termination of somatic hypermutation the selection rate s therefore has to decrease in order to prevent the GC reaction from growing. As discussed above the selection rate is believed to depend on the amount of available antigen and the behaviour can therefore best be modelled by again using a Hill function. Thus

$$s = s_c - h - f\frac{Ag_{min}^n}{Ag_{min}^n + Ag^n} \qquad \text{with} \quad Ag_{min} = 5000 \qquad n = 20. \tag{10}$$

We see that the selection rate is constant ($s = s_c$) for a large range of antigen densities but at a critical value of antigen availability the selection factor s falls rapidly to a constant value ($s = s_c - f$). Given that the selection factor is especially important in the time regime $t > 7$, the value of s_c is calculated with the parameters of this time regime ($p_r = 0.8, m = 0.72$) and we have $s_c = 0.45$. The parameter h needs to be introduced since the total B cell number decreases between day 7 and 16 when antigen consumption is not very important. Therefore the selection factor needs to be smaller than the equilibrium value of s and in order to reproduce the experimental data we chose $h = 0.07$. The factor f is needed in order to keep s

in the range [0, 1] and we chose $f = 0.35$ in order to reproduce the experimental data. The Hill coefficient for the recycling probability given in (8) can be reduced to $n = 20$.

The Hill coefficient n is a measure of the cooperativity of a process and a Hill coefficient of 3 is already considered high [38]. The reason such large values of the Hill coefficients had to be chosen in this model is that the selection rate and the recycling probability need to change rapidly and we see from Figure 2 that there is no alternative if we want to satisfy the kinetic data. We have therefore to assume that the fall of the selection factor is almost an on/off response where signalling is changed rapidly when the antigen density and affinity reaches a certain threshold. If we understand the rapid decrease in the selection proportion as an effect of a signalling cascade with many amplification steps a high Hill coefficient, which would not be justifiable for single molecule-molecule interactions, can still be realistic. Such a rapid change however makes the model very unstable against small variations in the initial conditions. When we include affinity maturation we will be able to model the selection factor and the recycling probability more mechanistically without having to use Hill functions, thus this problem will not arise.

The middle panel in Figure 2 shows the results of the model which compare even more closely with the experimental data [24] than the results in the top panel, which were obtained for continuous somatic hypermutation and constant selection rate. In the following we will always assume that somatic hypermutation terminates on about day 16 and we will see later that termination of somatic hypermutation by day 16 is also beneficial for the degree of affinity maturation, which further supports the idea of early termination of somatic hypermutation.

3.2 Centroblasts differentiate to centrocytes after one generation

After having introduced the basic model for one centroblast generation and having shown that it reproduces, reasonably well, kinetic data on the primed primary immune response, we now introduce a multi-generation model and show by comparison with experimental data that a one-generation model agrees best with experimental data. Up to day 3 the general multi-generation model is the same as before, but after day 3 it is given by

$$\frac{dB^0}{dt} = p_r \rho C_s - \rho B^0 \tag{11}$$

$$\frac{dB^j}{dt} = 2\rho m B^{j-1} - \rho B^j \qquad \text{for} \qquad j = 1, ..., n \tag{12}$$

$$\frac{dC}{dt} = 2\rho m B^n - \mu C \qquad \text{with} \quad \mu = ds + \delta_c(1-s) \tag{13}$$

$$\frac{dC_s}{dt} = dsC - \rho C_s \tag{14}$$

$$\frac{dM}{dt} = (1-p_r)\rho C_s \tag{15}$$

where the upper indices indicate the number of divisions the centroblast has already gone through. It is sufficient to numerically solve the problem for the one- and two-generation case in order to see why only the one-generation model is consistent with experimental data. While in this model centrocytes greatly outnumber centroblasts during the main part of the reaction (Figure 3(A)) as observed by MacLennan and coworkers [28], this is not the case in the two-generation model (Figure 3(B)). The

situation is even worse for more generations. Thus only the one-generation model is consistent with experimental observations.

3.3 Extension of the basic model to include affinity maturation

From the simple model for the GC reaction we now know that centroblasts probably differentiate into centrocytes after one cell division and that somatic hypermutation probably terminates around day 16. We now turn to modelling affinity maturation. Given that in the experimental work on affinity maturation on which we base this model only low, middle and high affinity clones are distinguished [36], it is sensible at this stage to restrict ourselves to two species, namely high and low affinity clones. We keep track of the cell populations in these affinity classes by using vectors of size two where the first argument refers to the number of cells with low affinity of the given cell species and the second argument to the number of cells with high affinity. The two components are denoted by subscripts. Mutation is modelled by applying a mutation matrix $\mathbf{M}$ and m is therefore replaced by $m\mathbf{M}$ in equation (2). Given that we assume somatic hypermutation to take place only between day 3.5 [26] and day 16 [5, 15] we have for $t \in [3.5, 16]$ $m = 0.72$ and $\mathbf{M}$ as given in equation (34). For all other times we have $m = 1$ and $\mathbf{M}$ the unit matrix. The constants differ for high and low affinity clones and are therefore written as pairs of numbers where the first argument refers to the constant for low affinity clones and the second argument to the constant for high affinity clones. In explicit form the system which we are going to solve looks as follows:

for $t \leq 3$

$$\frac{dB}{dt} = \rho B \tag{16}$$

for $t > 3$

$$\begin{aligned}
\frac{dB_1}{dt} &= p_{r_1}\rho C_{s_1} - \rho B_1 && (17)\\
\frac{dB_2}{dt} &= p_{r_2}\rho C_{s_2} - \rho B_2 && (18)\\
\frac{dC_1}{dt} &= 2\rho m(\mathbf{M}_{11}B_1 + \mathbf{M}_{12}B_2) - \mu_1 C_1 && (19)\\
\frac{dC_2}{dt} &= 2\rho m(\mathbf{M}_{21}B_1 + \mathbf{M}_{22}B_2) - \mu_2 C_2 && (20)\\
\frac{dC_{s_1}}{dt} &= ds_1 C_1 - \rho C_{s_1} && (21)\\
\frac{dC_{s_2}}{dt} &= ds_2 C_2 - \rho C_{s_2} && (22)\\
\frac{dM_1}{dt} &= (1 - p_{r_1})C_{s_1} && (23)\\
\frac{dM_2}{dt} &= (1 - p_{r_2})C_{s_2} && (24)
\end{aligned}$$

with $\mu_i = ds_i + \delta_c(1 - s_i)$.

The biological relevance of the different entries of $\mathbf{M}$ is as follows:

$\mathbf{M_{11}}$ - Proportion of low affinity cells that remain low affinity

$\mathbf{M_{12}}$ - Proportion of high affinity cells that become low affinity

$\mathbf{M_{21}}$ - Proportion of low affinity cells that become high affinity

$\mathbf{M_{22}}$ - Proportion of high affinity cells that remain high affinity

Given that the total number of cells does not change, the proportions need to sum to 1, so $\mathbf{M}_{11} + \mathbf{M}_{21} = 1$ and $\mathbf{M}_{12} + \mathbf{M}_{22} = 1$.

Affinity bins and mutation matrices have been used before in models of affinity maturation [17] although somatic hypermutation is believed to be a somewhat random process. The existence of hot spots [31] and the large number of cells justify a deterministic modelling approach. The use of affinity bins can be justified by the limited resolution of measurements.

3.3.1 Stability Analysis and the Possible Parameter Set of the selection factor s and the recycling probability p_r

In order to reproduce the experimental results the solution needs to tend to the trivial equilibrium point after day 4. The set of parameters for which this is achieved was determined by considering the quasistatic case when the selection rate s and the recycling probability p_r are constant and by then using the Routh-Hurwitz criterion. The possible parameter space is dependent on the proportion of beneficial mutations as can easily be seen in Figure 4 where the different parameter spaces for four different choices of $\mathbf{M}_{11}$ are depicted. The larger $\mathbf{M}_{11}$ the less restrictions lie on the parameters for high affinity clones (the selection probability s_2 and the recycling probability p_{r2}). This is also intuitively understandable since for large $\mathbf{M}_{11}$ only few high affinity clones are generated in every round of mutation and the population reducing effects therefore have to preferentially act on the low affinity population in order to prohibit the GC population from growing. We further see that high recycling rates are compatible with stable or falling population size if only a small proportion of all clones becomes selected as has already been observed in experiments.

3.3.2 Efficiency of affinity maturation

Given that the main focus of this paper is the process of affinity maturation it is now of interest to determine the restrictions on the parameters such that we indeed obtain affinity maturation.

We can analyse the efficiency of affinity maturation best by defining

$$\dot{T}_1 = \dot{B}_1 + \dot{C}_1 + \dot{C}_{s1} + \dot{M}_1 \tag{25}$$

$$\dot{T}_2 = \dot{B}_2 + \dot{C}_2 + \dot{C}_{s2} + \dot{M}_2. \tag{26}$$

so that T_1 (T_2) represents the rate of increase of low (high) affinity cells. We therefore have a net affinity increase if $\dot{T}_1 < \dot{T}_2$. This inequality is satisfied if the following conditions hold:

$$C_{s1} < C_{s2}\frac{1-p_{r2}}{1-p_{r1}} \tag{27}$$

$$C_1 > C_2\frac{1-s_2}{1-s_1} \tag{28}$$

$$\frac{B_1}{B_2} < \frac{-1+2m(\mathbf{M}_{22}-\mathbf{M}_{12})}{-1+2m(\mathbf{M}_{11}-\mathbf{M}_{21})} \tag{29}$$

From inequality (27) we see that affinity maturation is favoured if high affinity clones recycle with less probability than low affinity clones ($p_{r2} < p_{r1}$). We will come back to this idea soon when we analyse the mutation matrix in more detail. Inequality (28) yields the intuitively understandable insight that it is most beneficial

for affinity maturation if low affinity clones are selected to a lesser degree than high affinity clones ($s_1 < s_2$).

Inequality (29) can be further analysed by using $\mathbf{M}_{11}+\mathbf{M}_{21} = 1$, $\mathbf{M}_{12}+\mathbf{M}_{22} = 1$ and $\mathbf{M}_{21}+\mathbf{M}_{12} = \beta$ where β is the proportion of mutations that lead to an affinity change. We obtain from (29) the condition

$$\frac{B_1}{B_2} < \frac{-1+2m(3-2\beta-2\mathbf{M}_{11})}{-1+2m(2\mathbf{M}_{11}-1)}. \tag{30}$$

Given that the LHS of inequality (29) is bounded below by 0, we require the RHS to be larger than zero in order to obtain affinity maturation. This is achieved if either

$$\mathbf{M}_{11} > 0.5+0.25m^{-1} \quad \wedge \quad \beta < 1.5-0.25m^{-1}-\mathbf{M}_{11} \tag{31}$$

or

$$\mathbf{M}_{11} < 0.5+0.25m^{-1} \quad \wedge \quad \beta > 1.5-0.25m^{-1}-\mathbf{M}_{11} \tag{32}$$

Estimates by others yield $\beta = 0.52$ and $m = 0.72$ [34] and condition (31) can therefore not be satisfied, while condition (32) implies $\mathbf{M}_{11} < 0.85$ (Note that since (27)-(29) are sufficient but not necessary, the upper limit for $\mathbf{M}_{11}$ may in fact be higher). The RHS goes to zero when $\mathbf{M}_{11}$ approaches its upper limit and for large $\mathbf{M}_{11}$ we can therefore only obtain affinity maturation if the LHS can be made very small.

Obviously, there is a net shift of the mutation matrix $\mathbf{M}$ to high affinity if the population of low affinity centroblasts is larger than the population of high affinity centroblasts by more than $\frac{\mathbf{M}_{12}}{\mathbf{M}_{21}}$. One may be tempted to consider a model with several centroblast generations at this stage although we have previously ruled out such a model for kinetic reasons. Introduction of several centroblast generations leads to a multiple application of the matrix $\mathbf{M}$ on the centroblast vector while condition (29) is changed to

$$\frac{\sum_i B_1^i}{\sum_j B_2^j} < \frac{-1+2m(\mathbf{M}_{22}-\mathbf{M}_{12})}{-1+2m(\mathbf{M}_{11}-\mathbf{M}_{21})} = \frac{-1+2m(3-2\beta-2\mathbf{M}_{11})}{-1+2m(2\mathbf{M}_{11}-1)} \tag{33}$$

for $i,j = 1,..,n$ being the number of divisions the centroblasts have gone through. While the RHS is identical to the case for the one-generation model, the LHS of (33) now includes the sum of all centroblast populations.

Multiplication of the mutation matrix with itself however does not change the ratio $\frac{\mathbf{M}^n_{12}}{\mathbf{M}^n_{21}}$ as can be seen from the explicit calculation of $\mathbf{M}^n$ with $n = 2$

$$\mathbf{M}^2 = \begin{pmatrix} \mathbf{M}_{11}^2+\mathbf{M}_{12}\mathbf{M}_{21} & \mathbf{M}_{12}(\mathbf{M}_{11}+\mathbf{M}_{22}) \\ \mathbf{M}_{21}(\mathbf{M}_{11}+\mathbf{M}_{22}) & \mathbf{M}_{22}^2+\mathbf{M}_{12}\mathbf{M}_{21} \end{pmatrix}.$$

From this we see that the ratio between worsening and improving mutations is constant if the matrix is multiplied by itself. This implies that if the population of low affinity clones is larger than the population of high affinity clones by more than $\frac{\mathbf{M}_{12}}{\mathbf{M}_{21}}$ then we have a net increase in the high affinity population upon application of this matrix. If, however, the proportion of high affinity clones is higher, then this matrix lowers this proportion. In the limit we can therefore only attain the ratio $\frac{\mathbf{M}_{12}}{\mathbf{M}_{21}}$ by consecutive application of this matrix. This is illustrated in Figure 5, and we further see that the increase in the proportion of high affinity clones per application of the mutation matrix is highest when the proportion of high affinity clones is smallest and if n, the number of times the mutation matrix has already been applied, is small. This result is therefore also not in favor of a multi-generation model.

3.4 Termination of somatic hypermutation before the end of the GC reaction is beneficial for affinity maturation

In case of a termination of somatic hypermutation $\mathbf{M}$ becomes the unit matrix and (29) reduces to the inequality $\frac{B_1}{B_2} < 1$. This condition can be easily satisfied by introducing more stringent selection conditions which reduce the number of B_1 cells. The B_2 cells further multiply and soon dominate the germinal center reaction. From this it is obvious that it is beneficial to terminate somatic hypermutation before the germinal center reaction finishes in order to be able to further expand the high affinity clones without the risk of losing them because of worsening mutations. It is also clear that somatic hypermutation must not terminate before high affinity clones have evolved. Given that high affinity clones have about 9 mutations [35, 43], and assuming that one way through the cycle takes about a day, we need about 9 days of somatic hypermutation. Given that not every mutation is beneficial the 12 days allowed for somatic hypermutation to take place seem to be reasonable.

3.5 Numerical solution of the full model

After having gained insights concerning the number of centroblast generations, the time span of somatic hypermutation, the optimal choice of the selection factor and the recycling probability, the final step to take is to solve numerically the full model of the GC reaction including affinity maturation. Modelling affinity maturation allows us to finally include the competition between centrocytes and emerging high affinity antibodies as a driving force of affinity maturation. The resulting model is robust against variations in the initial antigen amount over several orders of magnitude and against variations in the proportion of beneficial mutations.

Below, biologically reasonable values are deduced for all parameters. In order to find the correct entries for $\mathbf{M}$ we use calculations by others [34] that estimate 53 % of all mutations to be silent and 28 % to be lethal. Therefore from the surviving 72 %, 74 % have not changed affinity while 26 % have. We cannot expect that more than 10 % of all mutations which change the affinity (or about 2 % of all mutations) are beneficial. Manser even assumes that only 0.1 % of all mutations are beneficial [29], a figure which may, however, be quite pessimistic. Assuming that 10 % of all changing mutations are beneficial we obtain as mutation matrix

$$\mathbf{M} = \begin{pmatrix} 0.948 & 0.468 \\ 0.052 & 0.532 \end{pmatrix} \tag{34}$$

which is derived as follows. If 10 % of all changing mutations were beneficial, 2.6 % of all low affinity clones would be promoted to high affinity in every round of mutation. We therefore have $\mathbf{M}_{21} = 0.1 \times 0.26 \times 2 = 0.052$ where the factor 2 comes in since the sum over all entries of $\mathbf{M}$ is 2. The remaining part of the low affinity clones remains of low affinity and we therefore find $\mathbf{M}_{11} = 1 - 0.052 = 0.948$. Given that we assume that 26 % of all mutations change the affinity, $(26 - 2.6)$ % = 23.4 % must reduce the affinity so that $\mathbf{M}_{12} = 0.234 \times 2 = 0.468$. The remaining high affinity clones remain of high affinity and we find for the last matrix entry $\mathbf{M}_{22} = 1 - 0.468 = 0.532$.

Given that the division rate is $\rho = \frac{24}{6.5}\, day^{-1}$ and we apply the mutation matrix continuously in every time step, we need to take $\mathbf{M}$ to the power $\frac{24\text{day}^{-1}}{6.5} \times dt$ with $dt = 0.1$ being our numerical finite time difference. Therefore, the actual value we take for the matrix $\mathbf{M}$ is:

$$\mathbf{M} = \begin{pmatrix} 0.9763 & 0.2136 \\ 0.0237 & 0.7864 \end{pmatrix}$$

These mutations change the proportion between high and low affinity clones, which is calculated from

$$\mathcal{A} = \frac{B_2 + C_2 + C_{s2} + M_2}{\sum_i (B_i + C_i + C_{si} + M_i)}. \tag{35}$$

Recall, that when we investigated the antigen dependency on the selection factor s and the recycling probability p_r in the previous section, we had to use unrealistically high values for the Hill coefficient n, and the basic model of the GC reaction was not robust to changes in the initial number of antigen complexes (a failing of the model since the amount of deposited antigen varies between GC reactions [26] and robustness of the real GC reaction to variations in several orders of magnitude has been observed). The GC reaction could attain such stability by a feedback mechanism such that in case of a high availability of antigen the total cell number would be reduced. A possible candidate for such a feedback mechanism is antigen masking by high affinity antibodies (Ab). On the other hand, antibodies with an affinity marginally above average may still be out-competed by centrocytes. The emergence of high affinity antibodies in the serum has been determined experimentally for a true primary immune response [36, 37]. The emergence of antibodies follows a saturation law and the largest increase in antibody concentration was found between day 7 (when high affinity antibodies can first be found) and day 14. A simplistic way of modelling the kinetics of high affinity antibody emergence is given by

$$\frac{dAb}{dt} = \kappa AFC_2 - fAgAb \qquad \text{with} \qquad \kappa = 0.5 \qquad f = 1.5 \times 10^{-4} \tag{36}$$

which is derived as follows. Given that high affinity antibodies are produced by high affinity plasma cells (AFC_2) it is sensible to assume that the increase in antibody concentration is proportional to the size of this cell population (first summand in (36)) while the decrease is proportional to antibody:antigen complex formation (second summand in (36)). The stochiometry of the complex depends on the antigen. Given that there is no data available on the amount of antibody found in GCs it is however not sensible to worry about stochiometries at this stage. With this model we can only investigate whether antigen masking by antibody could drive affinity maturation efficiently - further experiments are then needed to elucidate this point.

The availability of free, unbound antigen will decrease due to extraction as discussed before and due to antigen masking and we therefore have

$$\frac{dAg}{dt} = -(ukC + uC_s(1-k))Ag - fAgAb \qquad \text{with} \qquad f = 1.5 \times 10^{-4}. \tag{37}$$

Our choice of the selection factor s and the recycling probability p_r is guided by the analysis presented above. In order to gain maximal affinity increase we need to choose s_1 small while s_2 has to be large. The recycling probability, on the other hand, needs to be chosen high for low affinity clones (p_{r1}) and low for high affinity clones (p_{r2}). The recycling probability for high affinity clones has to increase with time, reflecting the stronger competition for activating signals because of reduction of available antigen. We therefore have

$$\mathbf{s} = \begin{pmatrix} 0.22(1 - 0.65\eta) \\ 0.95 \end{pmatrix} \tag{38}$$

$$\mathbf{p_r} = \begin{pmatrix} 0.25 + 0.7\zeta \\ 0.05 + 0.9\eta\zeta \end{pmatrix}$$

with $\zeta = \min\left(\frac{Ag}{1.2\sum_i C_i}, 1\right)$ and $\eta = \min\left(\frac{Ab}{Ag}, 1\right)$ where the exact values were chosen such that the kinetics are in close agreement with experimental data.

Termination of somatic hypermutation occurs at the same time at which selection stringency is increased. Both processes may therefore be regulated by the same mechanism and we assume that somatic hypermutation terminates when $\eta = 1$. A more realistic case would be a continuous decrease of somatic hypermutation with increasing η. Due to a lack of suitable parameters this cannot be expected to increase understanding of the process and would only change the model results in a way that leads to a smoothing of the region around $t = 16$ (see Figure 7 top panel).

The centrocytes which do not recycle can either differentiate into memory or antibody producing plasma cells (also called antibody forming cells (AFCs)). It has been observed that early selected centrocytes preferentially leave the GC reaction and differentiate into antibody forming cells, many of which migrate to the bone marrow where they persist for several weeks and secrete antibodies [36]. The proportion of high affinity clones among AFCs located in the spleen during the measurements has been determined explicitly in the experiments and we will use these data to validate the model.

There is inconclusive data concerning memory cells (M). While from histological investigations it was claimed that memory cells can first be found between day 3 and day 4 [26], investigations of the antibody repertoire support the concept that memory cells develop late during the response. Theoretical analysis shows that the affinity of the memory cell pool is higher the later memory cell formation starts [30] although at least in the model presented here the difference caused by a late start is not very high. *In vitro* experiments have shown that there may exist a feedback loop which inhibits plasma cell formation once there is a high titre of IgG antibodies [39]. In the true primary immune response they can be detected in the serum at day 7 [36, 37]. Taken together the dynamics of plasma and memory cells can be modelled by

$$\frac{dAFC}{dt} = \theta\rho(1-p_r)C_s \tag{39}$$

$$\frac{dM}{dt} = (1-\theta)\rho(1-p_r)C_s \tag{40}$$

where $\theta = \max(\frac{Ag-Ab}{Ag}, \alpha)$ is the fraction of free antigen and models the inhibition of AFC formation upon IgG development. The resulting kinetics are similar for $\alpha < 0.8$. For the numerical solution $\alpha = 0.3$ was chosen as a lower limit for θ since plasma cells still emerge late during the GC reaction so that to small values of α would be unrealistic.

Solving this system numerically yields the results shown in Figure 7. The overall kinetics behave as before and as described in the literature [24]. Given that we still work with a one-generation model, centrocytes still outnumber centroblasts as observed by MacLennan and coworkers [28]. While the total amount of antigen is only halved during the immune response ([40] and Figure 2), the amount of free antigen is reduced to zero during the response due to masking by soluble high affinity antibodies which are produced by plasma cells. This masking drives the competition in the germinal centres and leads to affinity maturation (Figure 7 middle panel) as observed in experiments [36]. The GC reaction and the affinity maturation in the model are very stable against increases in the initial amount of antigen over several orders of magnitude if measures are taken such that the number of antibodies cannot take negative values which would also be biologically unreasonable. This is in good agreement with the observation that the amount of deposited antigen varies [26] and experiments in which the antigen amount was strongly increased but

the reaction was found to be normal [42]. Also the proportion of beneficial mutations can be varied over a wide range without affecting the GC reaction or affinity maturation substantially. This robustness is very important since the proportion of beneficial mutations will strongly depend on the antigen encountered. In favour for the model is also the proportion of high affinity AFCs at day 14. Although nothing was specifically undertaken to influence this number, the proportion given in the literature (56%) [36] is reproduced well by the model (54%). The antibody level increases exponentially in this model while a saturation curve was obtained in the experiments [36]. The obvious reason for this is that in this model no further antibody decreasing processes such as the immune response against the invader are considered.

One further way to check the model is to impair recycling ($p_r = 0$). As has been shown experimentally [7] this leads to a break-down of the GC reaction (see Figure 8).

The last step is to build a multi-bin model. However, given that neither entries for the much more complex mutation matrix nor values for the different entries of s or p_r are known, it is sensible to wait for more experimental data to be available before undertaking a detailed modelling approach.

4 Discussion

4.1 Kinetic Aspects

a) Regulation of Centroblast to Centrocyte Differentiation: No experiments have been carried out to address the regulation mechanism for the differentiation of centroblasts into centrocytes. From the kinetic data available we can rule out either a cell density dependent or a time dependent mechanism. From the observation of MacLennan and coworkers [28] that centrocytes greatly outnumber centroblasts during the main part of the GC reaction it also follows that centroblasts differentiate into centrocytes after one cell division since otherwise both cell populations are either of the same size or centroblasts even outnumber centrocytes (see Figure 7). This result implies a much simpler mechanism for conversion than the model of Kesmir and de Boer [18] where it was proposed that centroblasts do not differentiate before having gone through at least 4 divisions, raising the question as to how centroblasts sense through how many generations they have already gone and whether somatic hypermutation acts on each generation.

b) Start of Memory Cell Formation: Recently a model has been proposed in which a non-output phase is shown to be beneficial for affinity maturation [30]. This leaves the question as to how the initiation of memory cell formation is regulated. If IgG at least partially inhibits AFC formation as measured *in vitro* [33, 39], memory cell formation may increase with time as was assumed in this model. Such a regulation would allow the body to produce antibodies as a first defense against rapidly dividing pathogens until the titre of high affinity IgG antibodies is sufficiently high and a feedback inhibition of AFC formation leads to a switch to more memory cell formation. AFCs and memory cells are also found in the bone marrow and other places in the body. It is however unknown which proportion emigrates and whether and how often cells divide before leaving the GC. Because of this lack of data emigration was not incorporated in the model.

There is a long-running debate on whether or not there is a further selection step for cells to either enter the memory or plasma cell pool [36]. There are certainly signals which bias selected centrocytes to differentiate in either direction [22] but given that the model presented here reproduces the experimental proportions of

high affinity clones without considering such a further selection step, properties other than affinity may be important for differentiation in either direction.

4.2 The Efficiency of Affinity Maturation

a) The role of Selection and Recycling: The process of immune response would be most efficient if somatic hypermutation worked on a small number of centroblast generations ($n < 10$) and if the initial and recycling centroblast population had a very small proportion of high affinity clones. This has indeed been shown for the initial centroblast population which was found to consist of 3 % high affinity clones [36]. In order to keep the proportion of high affinity centroblasts low, the recycling probability for high affinity centroblasts needs to be much smaller than for low affinity clones, which we already deduced from inequality (27). This is a new insight on the importance of this parameter for affinity maturation and raises the question of how high affinity clones could be generated from low affinity clones if clones of improved affinity hardly recycle and high affinity clones cannot be generated from low affinity clones in one round. This conceptual problem arises because of the simplicity of our model which only considers two different affinities so that a shift from low to high affinity *is* possible in this model.

At this stage it is therefore beneficial to consider an advanced model with 10 bins. The number 10 is sensible since experimentalists find that high affinity B cells differ in their antibody coding genes by about 8 mutations from germline genes. Assuming that every one of these mutations changes the affinity of the antibody it is sensible to use 8 bins for improved affinity, one for the starting affinity and one for reduced/no affinity. While cells below the starting bin undergo apoptosis when trying to interact with antigen, cells well above the starting bin are selected into the plasma cell pool or into the memory cell pool. The cells in the bins in between mostly recycle, some of them may also enter the memory pool. The threshold above which cells definitely leave the GC as memory or plasma cells can be assumed to increase during the germinal center reaction. This is in agreement with the analysis of the two bin model: once most of the population has gone say from bin 2 to bin 3, bin 3 acts as the low affinity bin in our model and is assigned the recycling probability for low affinity cells instead of that of high affinity cells. Therefore the recycling probability changes with time for the different bins and finally even clones of relatively high affinity recycle and are expanded. In this model, high affinity clones preferentially leave the GC reaction at the beginning. This is also intuitively understandable since at the beginning a high affinity clone, which was generated by chance, would be lost with high probability once it goes through mutation again since most of the mutations worsen the antibody. Additionally, the body needs early high affinity clones in order to hold the invader in check. Early emigration is therefore beneficial for the efficiency of affinity maturation and for the early immune response. Once, however, many clones have reached the next affinity bin and mutation acts on a wide platform, mutations are beneficial since they will not lead to a complete elimination of the already gained beneficial mutations but there is a good chance that affinity is even enhanced.

The early emigration of high affinity clones has been described previously [32, 36] but was understood to be due to a stochasticity in the selection and was viewed as a failure of the system [32]. The model presented here suggests that the early emigration is a deterministic process and is beneficial for affinity maturation and for the defence of the organism against the invader since the early emigrants produce antibodies which support the organism's first defence. This finding is also in good agreement with another experimental result where a transgene which coded for a high affinity antibody was inserted into the genome of an animal [41]. The animal nevertheless produced a similar memory cell repertoire as the control animals with-

out the transgene. This favours the notion of deterministic early emigration of high affinity clones which therefore do not dominate the response. In the later response animals without the transgene have obtained antibodies of comparable affinity by mutation while the antibody encoded by the transgene can accumulate worsening mutations.

The model also explains the results of Hannum and coworkers [10] which show that the germinal centre reaction is more or less normal even if the animals cannot deposit antigen on FDCs due to the lack of soluble antibodies. Their data shows that the GC cell numbers are even higher than in the control animals while the activation of centrocytes is less. Due to less activation, presumably more cells recycle and the GC reaction is therefore stable. The activation may be less since antigen cannot be displayed professionally on FDCs but needs to be recognised in other (maybe even in soluble) form which elicits less response [2].

The selection factor needs to be chosen in the opposite way to the recycling rate and is high for high affinity clones and low for low affinity clones. This is also intuitively understandable. With time competition for antigen increases because extraction of antigen by centrocytes lowers the antigen density. Therefore the selection proportion of low affinity clones decreases with time.

b) The role of termination of somatic hypermutation: The analysis of this model shows that termination of somatic hypermutation before the end of the germinal center reaction is beneficial for affinity maturation since it allows the expansion of high affinity clones without the hazard of losing the clone due to worsening mutations. The signal for a switch-off of somatic hypermutation may be less activation due to less availability of free antigen since this would also provide a mechanism for an increase in the selection stringency at the same time. The correlation may be due to a connection between activating signals during centrocyte selection and signals for continuation of somatic hypermutation after centrocytes have recycled. The signal may also be received directly by centroblasts which have been shown recently to express surface immunoglobulin in the late stages of the GC [6]. During that stage the dark and light zones can no longer be seen and the FDC network extends through the whole germinal centre such that centroblasts can directly interact with FDCs. These FDCs have further been shown to express CD23, also known as FcεRII, but not before the beginning of the second week of the response [6]. CD23 has been shown to bind to CD21, which modulates signalling through BCR. Such interactions may regulate somatic hypermutation termination.

In total we conclude that antigen masking by evolving antibody is an effective way by which affinity maturation may be driven. The postulated feedback effect on AFC formation may further regulate the extent to which B cells either leave the GC or recycle. Understanding the mechanism and regulation of recycling may be key to understanding affinity maturation as from this model the extent to which B cells leave or recycle has a very strong impact on affinity maturation. This is also sensible from a biological point of view since selection is mainly meant to have a protective function against the emergence of self-reactive clones. It is not sensible to eliminate even weak binders which can be used as plasma cells as a first defense against the invader. Furthermore the model strongly supports the concept of an early termination of somatic hypermutation at about day 16 since without such a termination affinity maturation would be less efficient and a need for more stringent selection conditions could not easily be reasoned. Termination of somatic hypermutation allows the expansion of the high affinity B cell population without the hazard of worsening mutations.

This model made use of several black boxes in which less well characterised steps were included. Before refining the model, predictions made by the model must be tested experimentally, and more data obtained on the dependence of B cell selection on BCR:antigen affinity and antigen density. Furthermore, it would be interesting to have data on the impact of antigen masking by antibody on affinity maturation and on fate determination by the quality of BCR:antigen and B cell: T cell interaction. Finally it would be helpful if the sizes of the different B cell populations (centroblasts, centrocytes, memory cells, plasma cells) were known in detail.

Acknowledgements DI would like to thank D. Gavaghan and M.C. MacLennan for useful discussions and acknowledges support from an EPSRC scholarship and the Studienstiftung des deutschen Volkes. This work was completed while PKM was a Visiting Senior Research Fellow at the Isaac Newton Institute for Mathematical Sciences, University of Cambridge.

References

[1] D. Allen, A. Cumano, R. Dildrop, C. Kocks, K. Rajewsky, N. Rajewsky, J. Roes, F. Sablitzky, and M. Siekevitz, *Timing, genetic requirements and functional consequences of somatic hypermutation during B cell development*, Immunol. Rev. **96** (1987), 5–22.

[2] F.D. Batista, D. Iber, and M.S. Neuberger, *B cells aquire antigen from target cells after synapse formation*, Nature **411** (2001), 489–494.

[3] F.D. Batista and M. Neuberger, *B cells extract and present immobilized antigen: implications for affinity discrimination.*, EMBO **19** (2000), 513–520.

[4] C. Berek, A. Berger, and M. Apel, *Maturation of the immune response in germinal centers*, Cell **67** (1991), 1121–1129.

[5] C. Berek and C. Milstein, *The dynamic nature of the antibody repertoire*, Immunological Reviews **105** (1988), 5–26.

[6] S.A. Camacho, M.H. Kosco-Vilbois, and C. Berek, *The dynamic structure of the germinal center*, Immunol Today **19** (1998), 511–4.

[7] C.G. de Vinuesa, M.C. Cook, J. Ball, M. Drew, Y. Sunners, M. Cascalho, M. Wabl, G.G.B. Klaus, and I.C. MacLennan, *Germinal centers without T cells*, J. Exp. Med. **191** (2000), 485–493.

[8] C.C.G. Goodnow, *Chance encounters and organized rendezvous*, Immunological Reviews **156** (1997), 5–10.

[9] S. Han, B. Zheng, J. DalPorto, and G. Kelsoe, *In situ studies of the primary immune response to (4-hydroxy-3-nitrophenyl)acetyl. iv. Affinity-dependent, antigen-driven B cell apoptosis in germinal centers as a mechanism for maintaining self-tolerance.*, J. Exp. Med. **182** (1995), 1635–1644.

[10] L.G. Hannum, A.M. Haberman, S.M. Anderson, and M.J. Shlomchik, *Germinal center initiation, variable gene region hypermutation, and mutant B cell selection without detectable immune complexes on follicular dendritic cells*, J. Exp. Med. **192** (2000), 931–942.

[11] D.L. Hardie, G.D. Johnson, M. Khan, and I.C. MacLennan, *Quantitative analysis of molecules which distinguish functional compartments within germinal centers.*, Eur J Immunol **23** (1993), 997–1004.

[12] J. Jacob, R. Kassir, and G. Kelsoe, *In situ studies of the primary immune response to (4-hydroxy-3-nitrophenyl)acetyl. I. the architecture and dynamics of responding cell populations*, J. Exp. Med. **173** (1991), 1165–1175.

[13] J. Jacob and G. Kelsoe, *In situ studies of the primary immune response to (4-hydroxy-3-nitrophenyl)acetyl. II. a common clonal origin for periarteriolar lymphoid sheath-associated foci and germinal centers*, J. Exp. Med. **176** (1992), 679–687.

[14] J. Jacob, G. Kelsoe, K. Rajewsky K, and U. Weiss, *Intraclonal generation of antibody mutants in germinal centres.*, Nature **354** (1991), 389–92.

[15] J. Jacob, J. Przylepa, C. Miller, and G. Kelsoe, *In situ studies of the primary immune response to (4-hydroxy-3-nitrophenyl)acetyl. III. the kinetics of V region mutation and selection in germinal center B cells*, J. Exp. Med. **178** (1993), 1293–1307.

[16] C.A. Janeway and P. Travers, *Immunology. the immune system in health and disease*, Garland Publisher, 1997.

[17] T.B. Kepler and A.S. Perelson, *Somatic hypermutation in B cells: an optimal control treatment*, J. Theor. Biol. **164** (1993), 37–64.

[18] C. Kesmir and R.J. de Boer, *A mathematical model on germinal center kinetics and termination*, Journal of Immunology **163** (1999), 2463–2469.

[19] F.G.M. Kroese, A.S. Wubena, H.G. Seijen, and P. Nieuwenhuis, *Germinal centers develop oligoclonally.*, Eur. J. Immunol. **17** (1987), 1069–1072.

[20] R. Kuppers, M. Zhao, M.-L. Hansmann, and K. Rajewsky, *Tracing B cell development in human germinal centres by molecular analysis of singel cells picked from histological sections*, EMBO **12** (1993), 4955–4967.

[21] A. Lanzavecchia, *Antigen-specific interaction between T and B cells*, Nature **314** (1985), 537–539.

[22] Y.J. Liu, O. de Bouteiller, and I. Fugier-Vivier, *Mechanisms of selection and differentiation in germinal centers.*, Curr Opin Immunol **9** (1997), 256–62.

[23] Y.L. Liu, D.E. Joshua, C.A.G.J. Smith, and I.C. MacLennan, *Mechanisms of antigen-driven selection in germinal centres*, Nature **342** (1989), 929–931.

[24] Y.L. Liu, J. Zhang, E.Y.T. Chan, and I.C. MacLennan, *Sites of specific B cell activation in primary and secondary responses to T-cell-dependent and T-cell-independent antigens*, Eur J Immunol **21** (1991), 2951–2962.

[25] I.C. MacLennan, *Germinal centers*, Annu. Rev. Immunol. **12** (1994), 117–139.

[26] ———, personal communication (2001).

[27] I.C. MacLennan, C. Garciá de Vinuesa, and M. Casamayor-Palleja, *B-cell memory and the persistence of antibody responses.*, Philos Trans R Soc Lond B Biol Sci. **355** (2000), 345–350.

[28] I.C. MacLennan, Y.L. Liu, S. Oldfield, J. Zhang, and P.J.L. Lane, *The evolution of B-cell clones.*, Curr Top Microbiol Immunol **159** (1990), 37–64.

[29] T. Manser, *The efficiency of antibody affinity maturation: can the rate of B-cell division be limiting?*, Immunology Today **11** (1990), 305–308.

[30] M. Meyer-Hermann, A. Deutsch, and M. Or-Guil, *Recycling probability and dynamical properties of germinal center reactions*, J Theor Biol **210** (2001), 265–285.

[31] M.S. Neuberger, M.R. Ehrenstein, N. Klix, C.J. Jolly, J. Yelamos, C. Rada, and C. Milstein, *Monitoring and interpreting the intrinsic features of somatic hypermutation.*, Immunol Rev **162** (1998), 107–16.

[32] M.D. Radmacher, G. Kelsoe, and T.B. Kepler, *Predicted and inferred waiting times for key mutants in the germinal centre reaction: Evidence for stochasticity in selection*, Immunology and Cell Biology **76** (1998), 373–381.

[33] A. Ridderstad and D.M. Tarlinton, *Kinetics of establishing the memory B cell population as revealed by CD38 expression*, J. Immunol. **160** (1998), 4688–4695.

[34] M. Shannon and R. Mehr, *Reconciling repertoire shift with affinity maturation: The role of deleterious mutations*, Journal of Immunology **162** (1999), 3950–3956.

[35] M. Siekevitz, C. Kocks, K. Rajewsky, and R. Dildrop, *Analysis of somatic mutations and class switching in naive and memory B cells generating adoptive primary and secondary responses*, Cell **48** (1987), 757–770.

[36] K.G.C. Smith, A. Light, G.J.V. Nossal, and D.M. Tarlinton, *The extent of affintiy maturation differs between the memory and antibody-forming cell compartments in the primary immune response*, EMBO **16** (1997), 2996–3006.

[37] K.G.C. Smith, U. Weiss, K. Rajewski, G.J.V. Nossal, and D.M. Tarlinton, *Bcl-2 increases memory B cell recruitment but does not perturb selection in the germinal centers*, Immunity **1** (1994), 803–813.

[38] L. Stryer, *Biochemistry*, W.H. Freeman and Company, 1995.

[39] D.M. Tarlinton and K.G.C. Smith, *Dissecting affinity maturation: a model explaining selection of antibody-forming cells and memory B cells in the germinal centre*, Immunol Today **9** (2000), 436–441.

[40] J.G. Tew and T.E. Mandel, *Prolonged antigen half-life in the lymphoid follicles of specifically immunized mice*, Immunology **37** (1979), 69–76.

[41] K.A. Vora and T. Manser, *Altering the antibody repertoire via transgene homologous recombination: evidence for global and clone-autonomous regulation of antigen-driven B cell differentiation*, J Exp Med **181** (1995), 271–281.

[42] K.A. Vora, J.V. Ravetch, and T. Manser, *Amplified follicular immune complex deposition in mice lacking the Fc receptor γ-chain does not alter maturation of the B cell response*, J Immunol **159** (1997), 2116–2124.

[43] G.J. Wedemayer, P.A. Patten, L.H. Wang, P.G. Schultz, and R.C. Stevens, *Structural insights into the evolution of an antibody combining site.*, Science **276** (1997), 1665–9.

Table 1: GC kinetics in the primed primary immune response

days	Action	References
1	immunisation	
first 3	B blast proliferation with 1 division within 6-7 hours	[24]
3	first apoptosis (no memory cells yet)	[26]
3 - 4	differentiation of B blasts into centroblasts,	[24]
	onset of somatic hypermutation	
	(at 96 hours already two generations of mutations)	[26]
	start of memory cell formation	[24], [26]
4	GC formation: centroblast (dark zone) and centrocytes (light zone)	[12], [13], [24]
	GC biggest now	[24]
5	mutated plasma cells can be found (may have already appeared earlier)	[26]
21	GC reaction finishes	[12], [13], [24]

Table 2: Parameters for the minimal model

B	centroblasts	
C	centrocytes	
C_s	centrocytes that have been selected	
M	memory cells	
$\rho = \frac{24}{6.5} \ln 2$	maximum proliferation rate of centroblast (day^{-1})	[24]
$m = 0.72$	probability of non-deleterious mutation	[34]
$d = 12 \ln 2$	rate of running through the selection process ($\text{day}^{-}1$)	[24]
$\delta_c = 1.5 \ln 2$	death rate of centrocytes	[28]
$s \in [0, 1]$	selection probability of centrocytes	
$p_r \in [0, 1]$	probability of recycling	

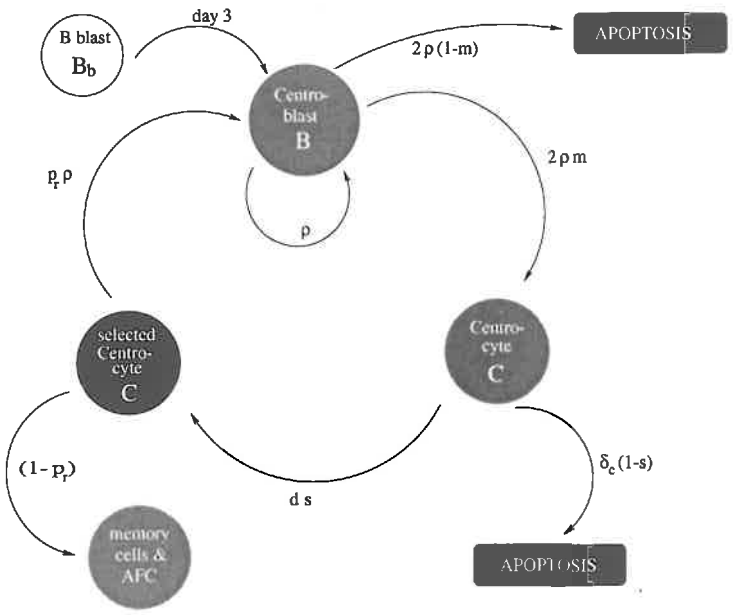

Figure 1: Scheme of the model for the primed primary immune response. Abbreviations are explained in Table 2.

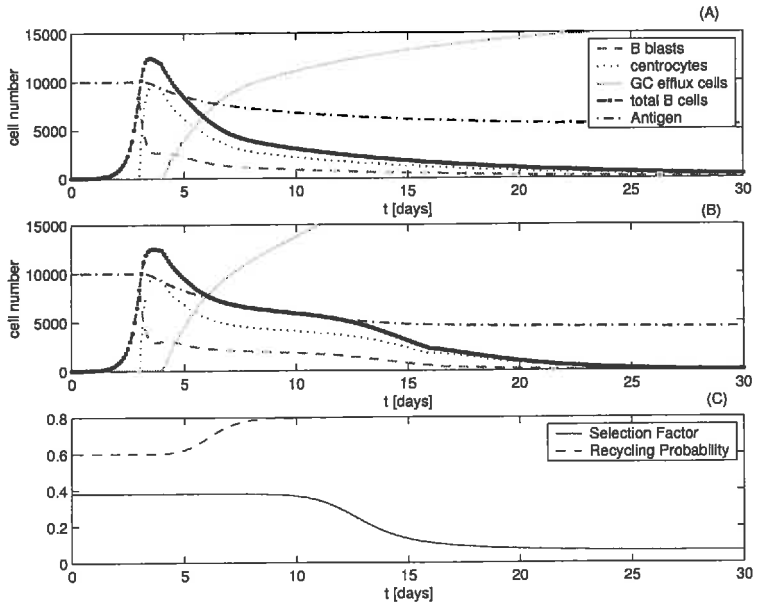

Figure 2: (A) GC kinetics without termination of somatic hypermutation. The recycling probability is chosen as given in (8). The selection factor $s = 0.28$ is chosen constant. (B) GC kinetics with termination of somatic hypermutation at day 16. The final number of GC efflux cells is 2.1×10^4. The recycling probability used is given in (8) with $n = 20$, and the selection rate is given in (10). (C) The selection factor s and the recycling probability p_r as in (B).

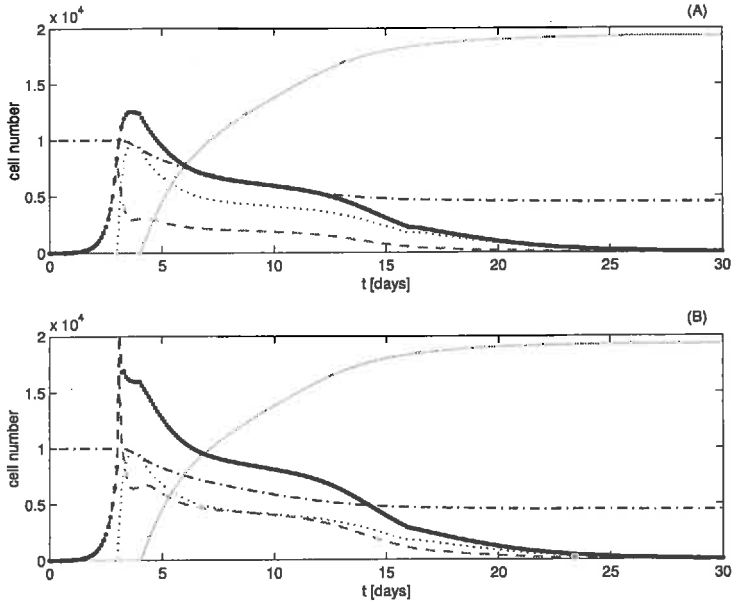

Figure 3: GC kinetics of the primed primary immune response in the one-generation model where selection (s) and recycling (p_r) is dependent on antigen density, and somatic hypermutation terminates at day 16. (A) One-generation model: The dynamics of all cell populations behave as described before. (B) Two-generation model: The dynamics of all cell populations behave as described before except that the centroblast and the centrocyte population are of similar size.

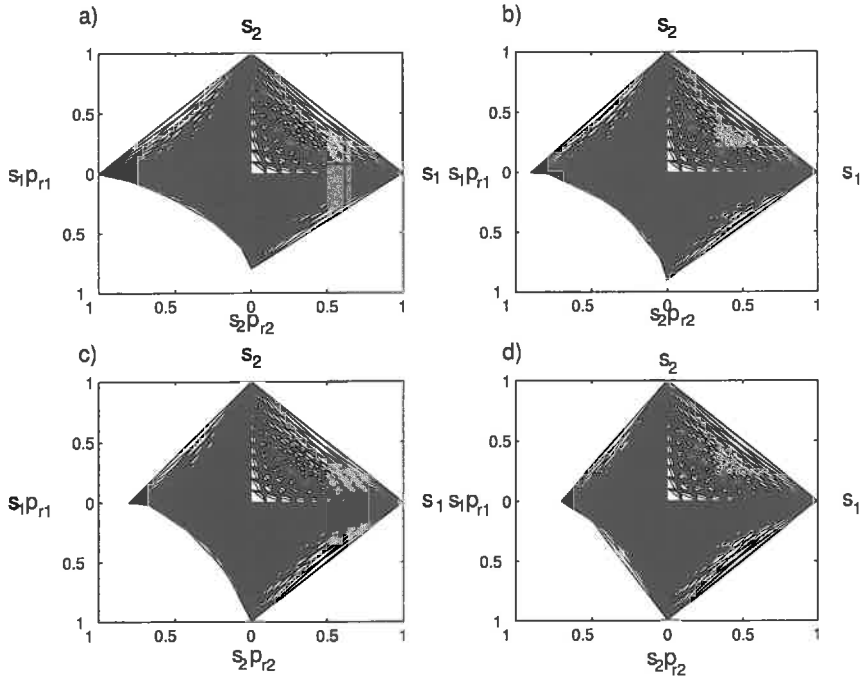

Figure 4: Parameter space for which system attains the trivial equilibrium point *a)* M_{11} = 0.65; *b)* M_{11} = 0.75; *c)* M_{11} = 0.85; *d)* M_{11} = 0.95

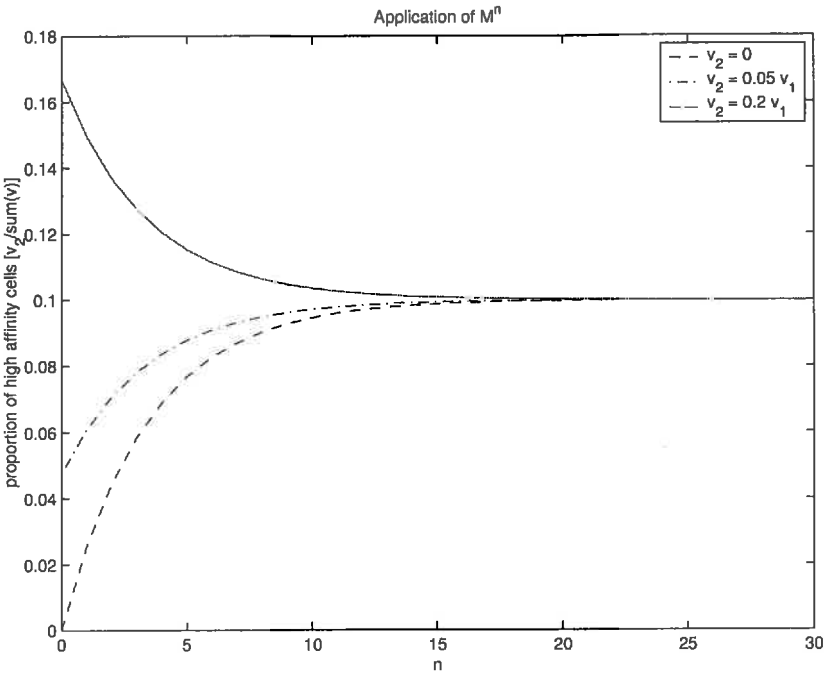

Figure 5: Consecutive application of the mutation matrix M: The proportion of high affinity cells $\frac{v_2}{\sum_i v_i}$ is plotted against the number of times n the mutation matrix M was applied. The shift per application of the mutation matrix depends on the initial proportion of high affinity cells, v_2, given in the legend in the inset.

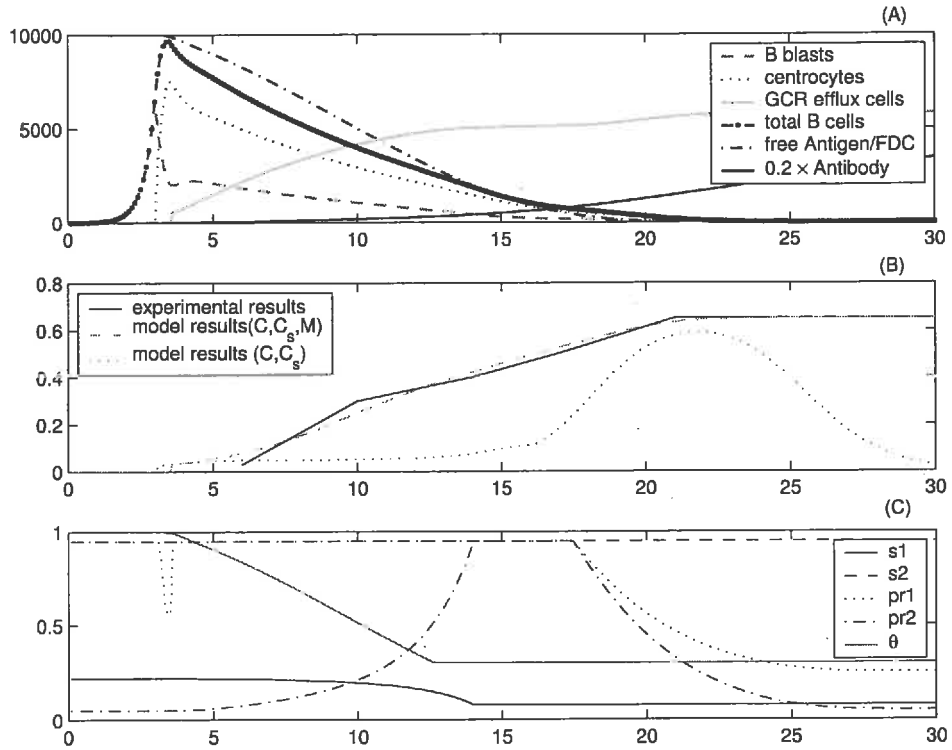

Figure 6: GC kinetics and affinity maturation of the primed primary immune response without termination of somatic hypermutation. (A) GC kinetics of the primed primary immune response in the one-generation model. The dynamics of all cell populations behave as described before. (B) Affinity maturation during the primed primary immune response: The model results are close to those observed experimentally. The earlier onset of affinity maturation seen in the model results derives from the nature of the primed primary immune response. The experimental results were obtained for a true primary immune response [36] which starts later than the primed primary immune response. (C) The dynamic behaviour of the selection and recycling probability for low and high affinity clones is depicted as well as θ, the fraction of free antigen.

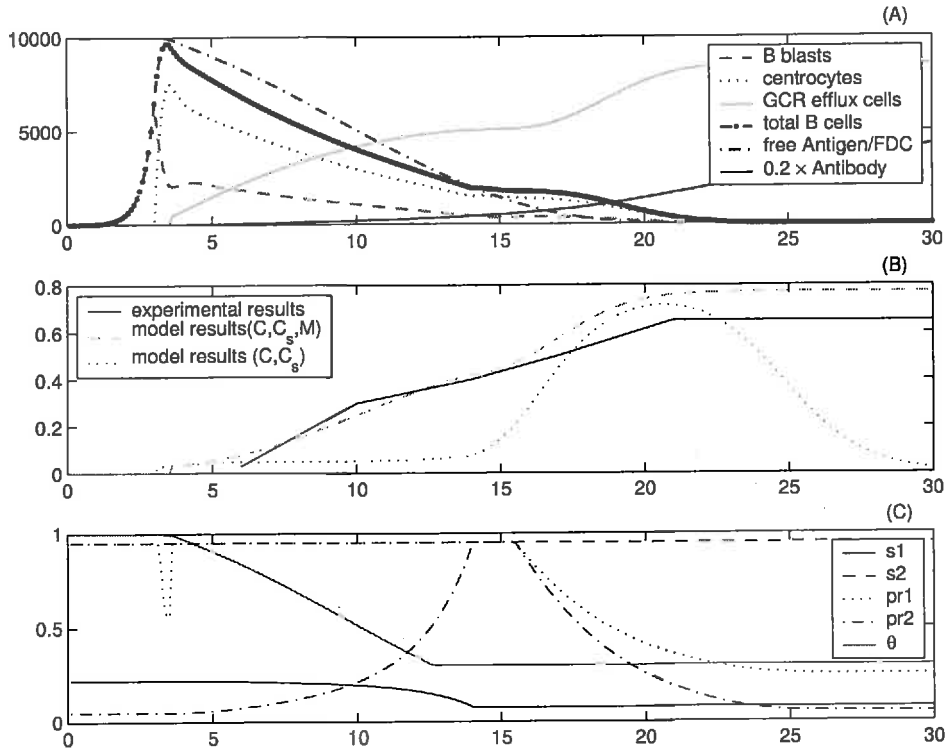

Figure 7: GC kinetics and affinity maturation of the primed primary immune response if somatic hypermutation terminates before the end of the GC reaction. (A) GC kinetics of the primed primary immune response in the one-generation model. The dynamics of all cell populations behave as described before. (B) Affinity maturation during the primed primary immune response: The model results are similar to the experimental results except for the final affinity increase after day 16. Until about day 16 the affinity increase is largely due to an affinity increase in the memory population. After the termination of somatic hypermutation the average affinity increases again substantially due to an affinity increase in the centrocyte population. Termination of somatic hypermutation before the end of the GC reaction is therefore beneficial for affinity maturation and would be necessary to reproduce experimental data if a lower proportion of improving mutations had been chosen. (C) The dynamic behaviour of the selection and recycling probability for low and high affinity clones is depicted as well as θ, the fraction of free antigen.

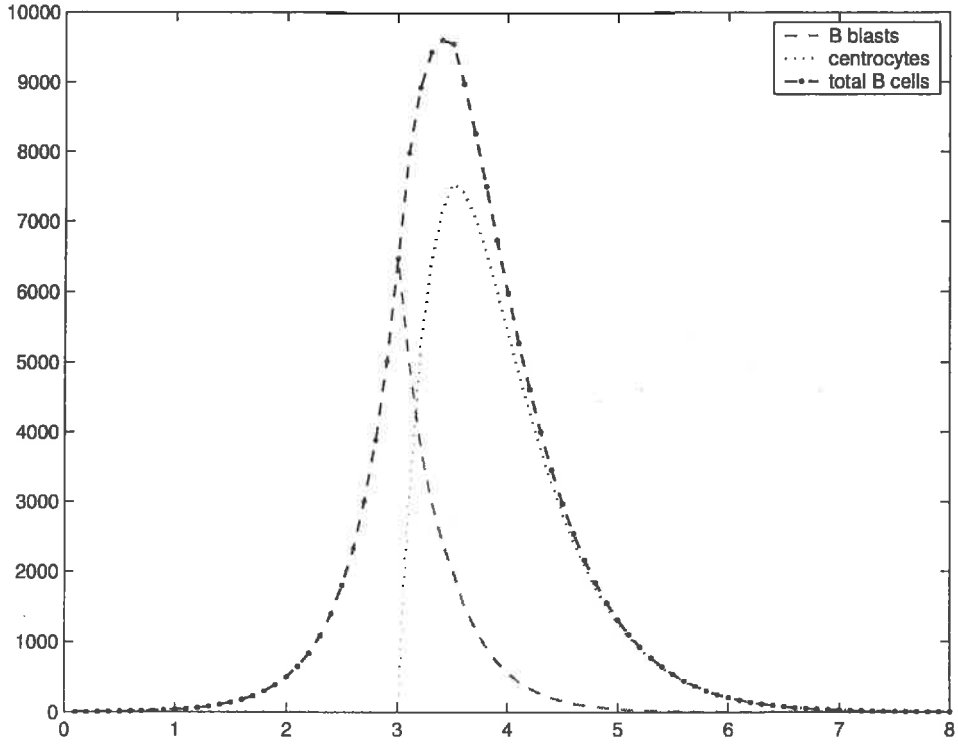

Figure 8: GC kinetics during the primed primary immune response if recycling is impaired as observed in experiments [7]: the GC reaction breaks down between day 5 and 6 of the response.